Electronic Supplementary Material (ESI) for Nanoscale.
This journal is © The Royal Society of Chemistry 2015

Electronic Supplementary Information

S1. Synthesis of PLGA-RHO

The preparation of PLGA-RHO conjugate was performed under inert nitrogen or argon atmosphere and dry conditions according to scheme 1.

The preparation of PLGA-Rhodamine conjugate was performed under inert nitrogen or argon atmosphere and dry conditions.

1. c-PLGA502H-N_3(figure S1.1): The terminal hydroxyl group of PLGA502H was changed into azide by two-step azidation with mesyl chloride activation. After 24 hours reaction mixture was simply concentrated and precipitated in diethyl ether methanol solution 1/1 v/v obtaining a sponge like solid. Thereafter, nucleophilic substitution with sodium azide was carried out in DMF/water solution (20/1 v/v) and temperature was set at 38°C for 24 hours. Reaction mixture was dried, redissolved in $CHCl_3$,filtered and precipitated in diethyl ether.

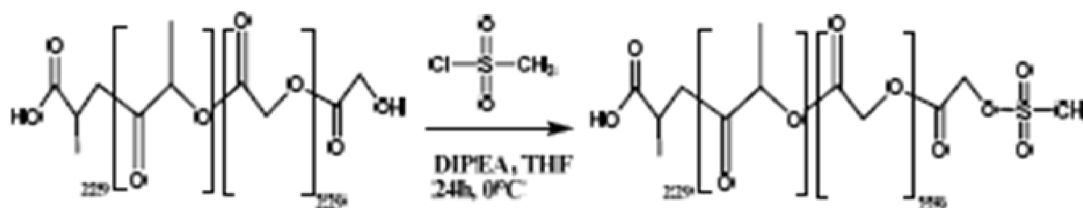

Scheme S1.1. c-PLGA502H-OH hydroxyl activation with mesyl chloride.

^{1}H-NMR analysis was used to confirm product chemical structure. As illustrated in figure S1.2A, in the ^{1}H-NMR spectrum of c-PLGA502H-OH, a-hydroxyl methylene (d) is quite visible at 4.31 ppm and is possible to adopt this signal as diagnostic standard for further reaction. NMR spectrum of c-PLGA502H-mesyl (figure S1.2B) was analyzed, comparing integration values of the signals related to the protons CH_3-CH- (a) (δ =1.60) and terminal CH_3-OSO (e) (δ = 3.21). The conversion degree is higher than 95%. Other evidence of quantitative reaction is total disappearance of signal at 4.31 ppm related to α-hydroxyl methylene.

The reaction grade of nucleophilic addition to give c-PLGA502H-N_3, was evaluated comparing integrations values of the signals related to the protons CH3-CH- (a) (δ = 1.60) and terminal CH_2-N_3 (d) (δ = 4.30) (figure S1.2C). The conversion degree of c-PLGA502H-mesyl, within the limits of experimental error, was higher than 95%. Other evidence of quantitative reaction is the total disappearance of signal at 3.21 ppm related to mesyl group.

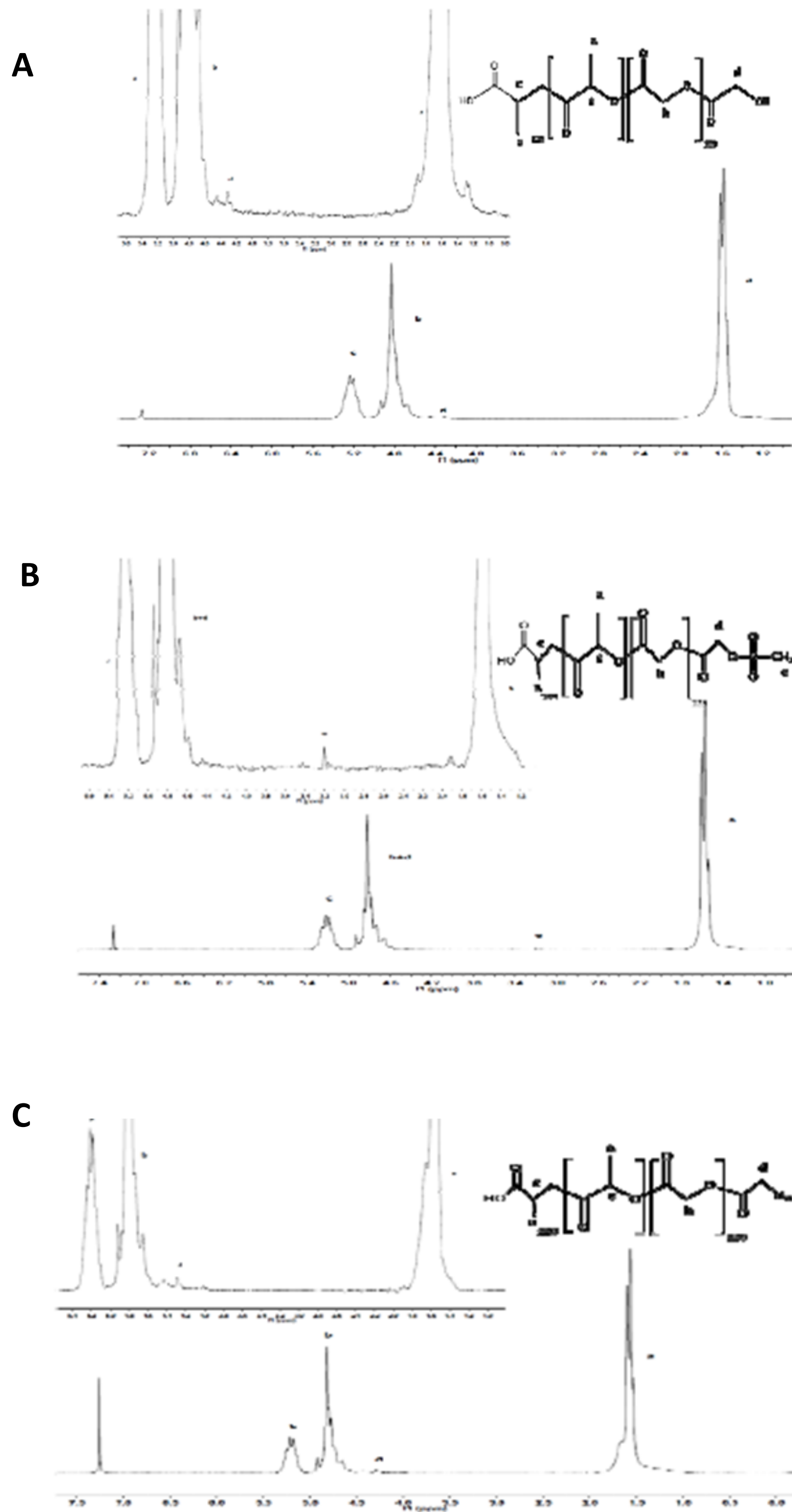

Figure S1.2. ^{1}H-NMR of *A)* c-PLGA502H-OH; B) c-PLGA502H-mesyl; C) c-PLGA502H-N_3 with proton assignment.

Also FTIR analysis shows clearly diagnostic stretching signal of azide at 2100 cm-1 (Figure S1.3).

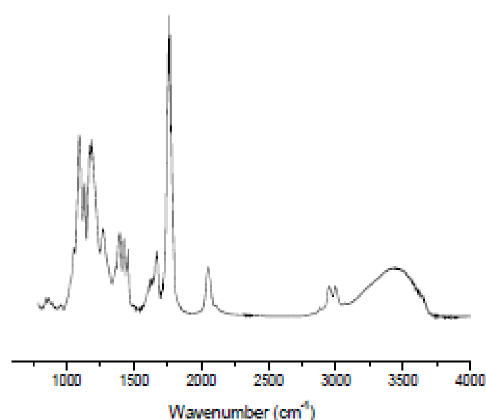

Figure S1.3. FTIR spectrum of c-PLGA502H-N_3.

2. *Rhodamine coupling with* c-PLGA502H-N_3 (figure S1.4A):Rhodamine B was reacted with 3-Butynol in presence of DCC and DMAP to give alkyne ester. After 48 h reaction mixture was filtered from dicyclohexylurea, concentrated and purified by silica gel chromatography with $CHCl_3$/Methanol 9/1 v/v as eluent. Thereafter, the Huysgen cycloaddition between Rhodamine-alkyne and c-PLGA502H-N_3 was carried out (figure S1.4B) in 30% molar excess of Rhodamine-alkyne and cocatalyst N,N-Diisopropylethylamine (DIPEA), in 5/1 molar ratio between c-PLGA502H-N3 and the catalyst $[(Ph)_3P]_3CuBr$. After 48 h stirring at 35°C, reaction mixture was concentrated, purified by Cu(I) catalyst by neutral alumina column and precipitated in diethyl ether methanol solution 1/1 v/v.

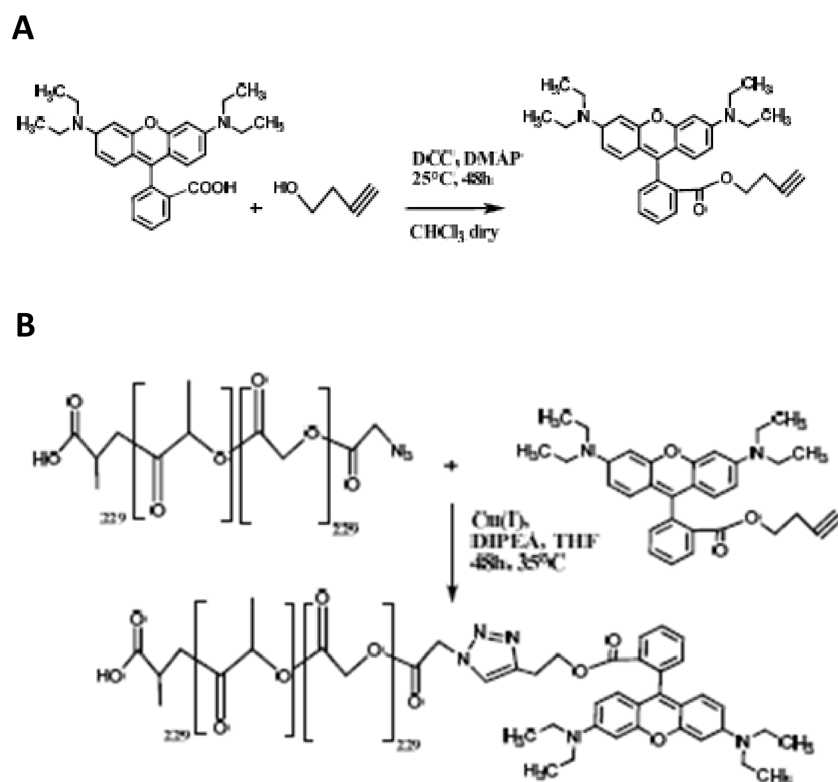

Figure S1.4. A) reaction between Rhodamine B and 3-Butynol to give Rhodamine-alkyne; B) Huysgen cycloaddition between Rhodamine-alkyne and c-PLGA502H-N_3 to give final fluorescent polymer (PLGA-RHO).

^{1}H-NMR analysis was first used to confirm product chemical structure, Rhodamine-alkyne, comparing integrations values of the signals related to the protons CH3-CH- (a) (δ = 1.60) and terminal CH_2-O-CO (d) (δ = 4.30) (figure S1.5A) was evaluated that Rhodamine B conversion degree is higher than 95%.

The reaction grade Huisgen Cycloaddition to give c-PLGA502H-Rhodamine was evaluated, comparing integrations values of the signals related to the protons CH_3-CH- (a) (δ = 1.60) and terminal CH_2-O-CO (n) (δ = 4.20) (figure S1.5B) The final c-PLGA502H-N_3 conversion degree is, within the limits of experimental error, higher than 95%.

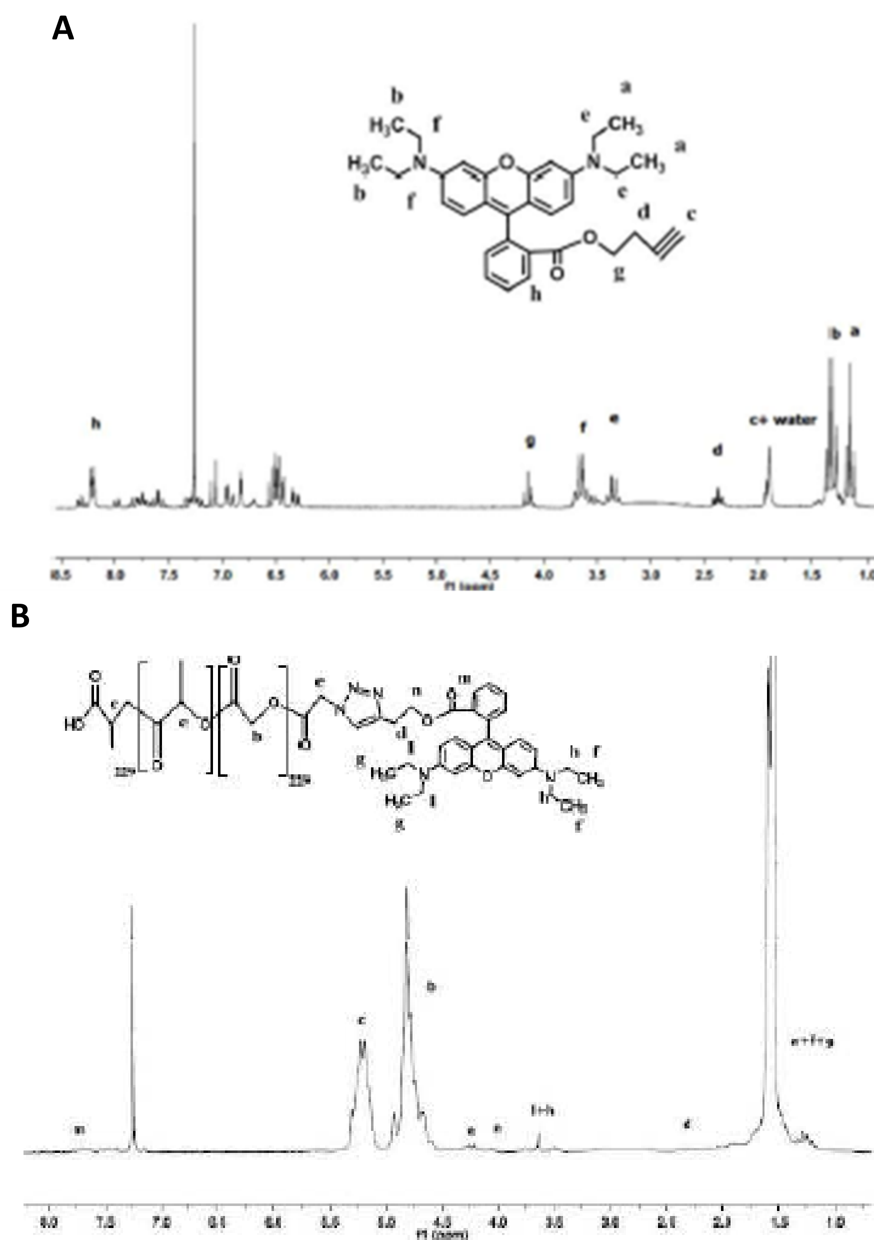

Figure S1.5. ^{1}H-NMR of A) Rhodamine-alkyne; B) c-PLGA502H-Rhodamine with proton assignment.

FTIR confirm quantitative coupling; can be noted, in fact, complete disappearance of diagnostic stretching signal of azide at 2100 cm^{-1} (Figure S1.6).

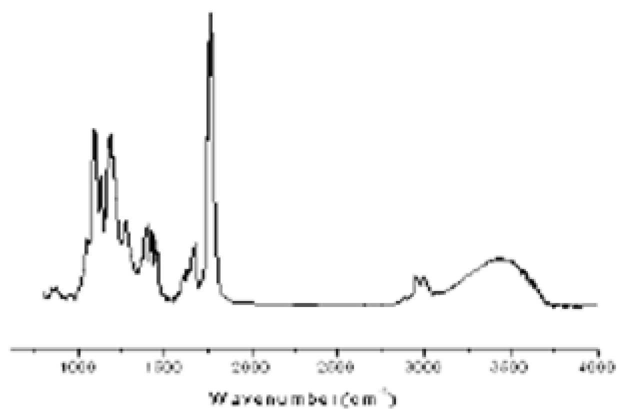

Figure S1.6. FTIR spectrum of c-PLGA502H-Rhodamine.

S2. Stability of DTX/TPPS$_4$-dcNPs in different media.

Freeze-dried DTX/TPPS$_4$-dcNPs were dispersed in water, DMEM FBS- and DMEM FBS+.Hydrodynamic diameter,polydispersity index (PI) and zeta potential of NPs after each preparation step were determined on a ZetasizerNano Z (Malvern Instruments Ltd., UK). Results are reported as mean of three separate measurements of three different batches (n=9) ± SD.

Absorption spectra of freeze-dried DTX/TPPS$_4$-dcNPs dispersed in water was recorded on a UV 1800 (Shimadzu, Japan) using a 1 cm pathlength quartz cell.

As shown in Table S2, a slight size growth is observedin DMEM FBS- which becomes more marked in DMEM FBS+. In all the cases, no macroscopic aggregation of DTX/TPPS$_4$-dcNPs is observed. Nevertheless, zeta potential is decreased in the media tested and remains unaltered independently of the presence of proteins.

Table S2. Properties of freeze-dried DTX/TPPS$_4$-dcNPs in different media.

	Size nm	**PI**	**Zeta potential mV**
Water	203 ± 10	0.15	-22
DMEM FBS-	244 ± 28	0.26	-9.5
DMEM FBS+	328 ± 10	0.27	-10.0

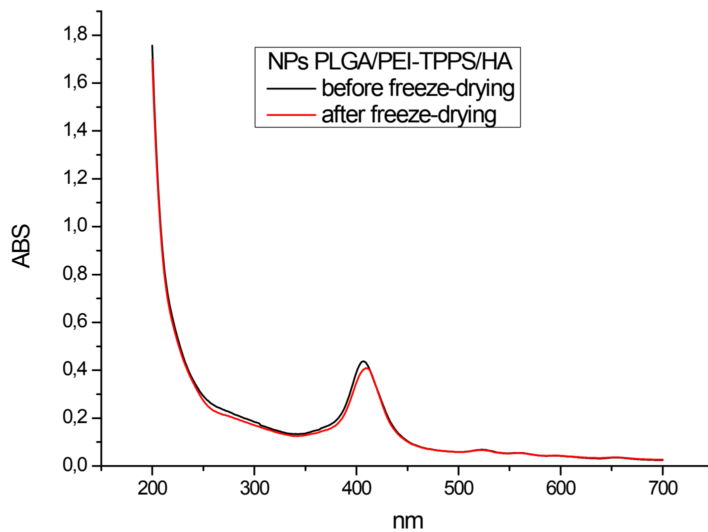

Figure S2. Absorption spectra of DTX/TPPS-dcNPsin water before and after freeze-drying.

S3. Intracellular localization of NPs

The intracellular localization of $TPPS_4$, free and in nanoparticles ($TPPS_4$-dcNPs) was determined by confocal microscopy. MDA-MB231 cells (6×10^4), seeded in special tissue culture dishes for fluorescence microscopy (µ-Dish $^{35mm, high}$, Ibidi GmbH, Planneg, Germany), wereallowed to growth for 24 h and then incubated for 24 h with 1 µg/mL PS diluted in medium added with 3% FBS. Fifteen min before the end of the incubation with the PS, the cells were stained with BODIPY® FL C_5-Ceramide (15 µM) orLysoTracker® Green DND-26 (75 nM) used as markers for Golgi apparatus and lysosomes, respectively. Cells were then washed twice with PBS with Ca^{2+} and Mg^{2+}andimmediately analyzed with a Leica SP5 confocal laser-scanning microscope (Leica Microsystems Srl, Milan, Italy); the images were elaborated with the ImageJ software.

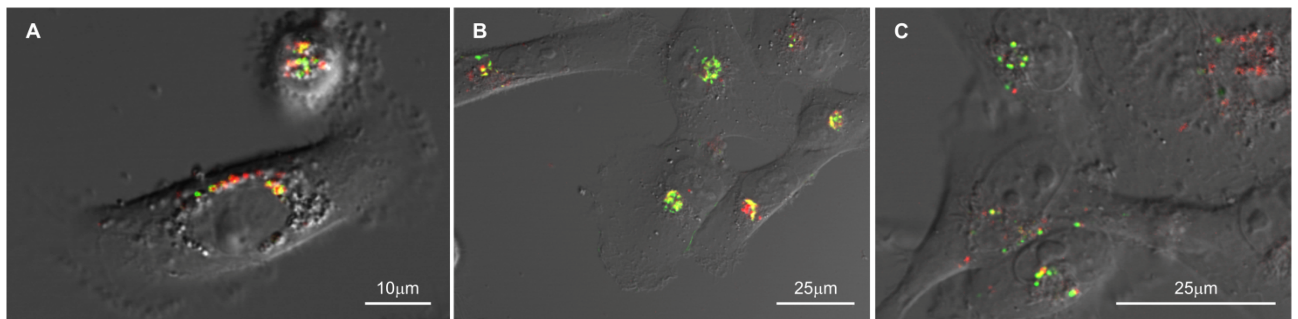

Figure S3. Confocal microscopy images showing the intracellular localization of $TPPS_4$-dcNPs (A) and free $TPPS_4$ (B, C) in MDA-MB-231 cells incubated for 24 h. A and C: merged images of $TPPS_4$and LysoTracker green; B: merged images of $TPPS_4$andBODIPY® FL C5-ceramide.

S4. Cell cycle analysis

MDA-MB231 cells (1×10^6) were seeded in 100 mm culture dishes and incubated with free DTX or DTX NPs for 24 h. Treated and control cells were harvested, fixed in 70% cold ethanol and stored at 4 °C overnight. Before analysis, cells were washed in distilled water, centrifuged and resuspended in 1 mL PBS containing 50 µg/mLpropidium iodide (Sigma-Aldrich) and 100 µg/mLRNAse, for DNA staining. Samples were incubated for 1 h at 37 °C and then analyzed by flow cytometry. Data from 2×10^4 cells/sample were acquired with the FACSDivasoftware and analyzed with the ModFit LT 3.0 software (BD Biosciences) to determine alterations in cell cycle distribution.

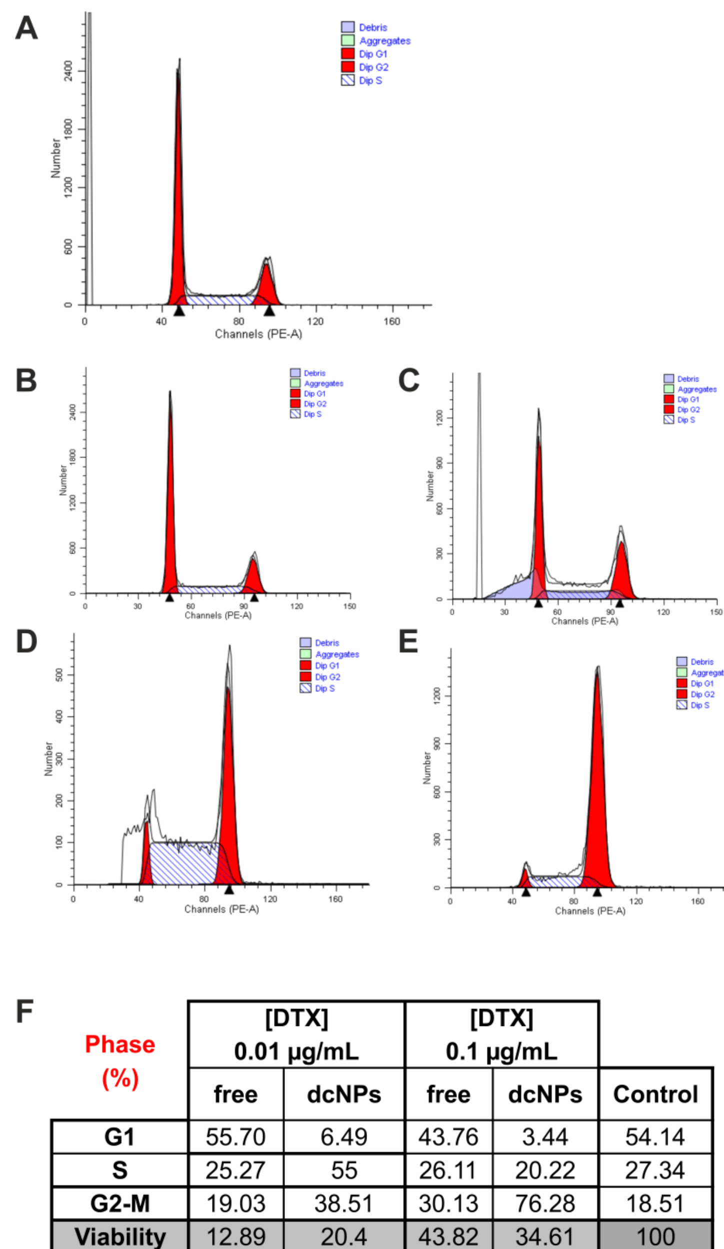

Phase (%)	[DTX] 0.01 µg/mL		[DTX] 0.1 µg/mL		
	free	dcNPs	free	dcNPs	Control
G1	55.70	6.49	43.76	3.44	54.14
S	25.27	55	26.11	20.22	27.34
G2-M	19.03	38.51	30.13	76.28	18.51
Viability	12.89	20.4	43.82	34.61	100

Figure S4. Analysis of cell cycle of MDA-MB-231 cells exposed to free DTX or DTX-dcNPs for 24 h. Control cellsA); cells exposed to free DTX at 0.01 µg/mLB) or 0.1 µg/mL D); cells exposed to DTX-dcNPs at 0.01 µg/mLC) or 0.1 µg/mL E). Percentages of cells the various phases are shown in F).

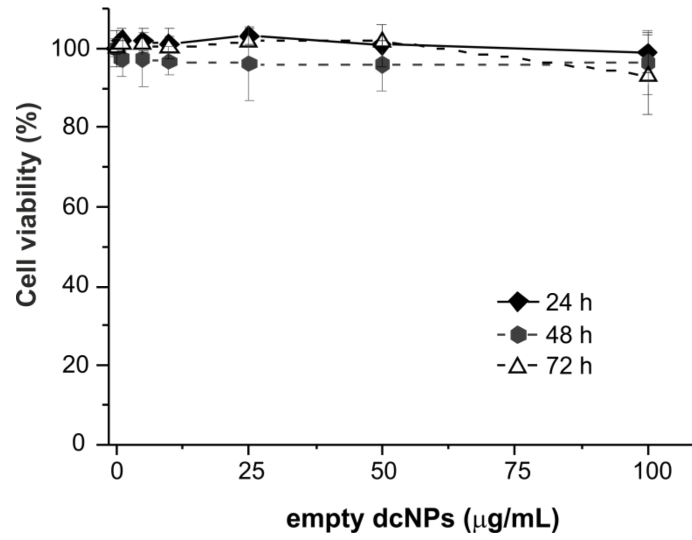

Figure S5. Cell viability of MDA-MB-231 cells exposed up to 72 h to increasing concentrations of empty dcNPs.

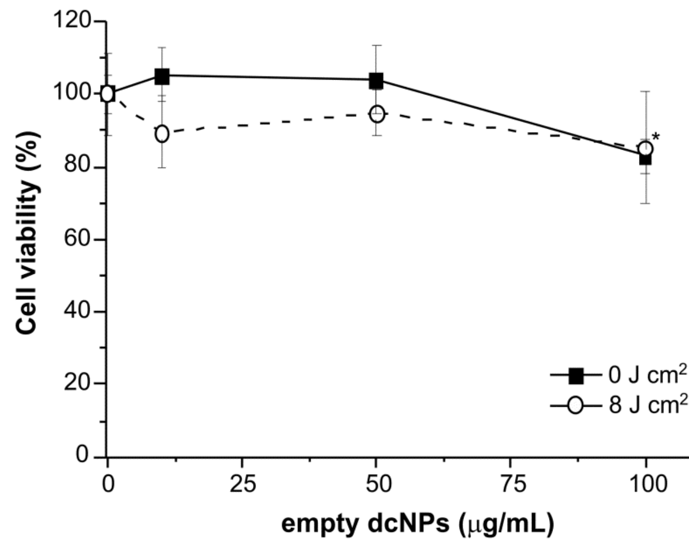

Figure S6. Viability of MDA-MB-231 cells exposed for 24 h to increasing concentrations of empty dcNPs and kept for additional 24 h in complete medium after being or not exposed to 8 J/cm^2 of blue light.